ELSEVIER

Polymer 40 (1999) 3309–3322

polymer

High-resolution solid-state ^{13}C n.m.r. study on phase structure of the compositionally fractionated bacterial copolyester poly(3-hydroxybutyric acid-co-3-hydroxypropionic acid)s

Amin Cao, Naoki Asakawa, Naoko Yoshie, Yoshio Inoue*

Department of Biomolecular Engineering, Tokyo Institute of Technology, 4259 Nagatsuta, Midori-ku, Yokohama 226-8501, Japan

Received 9 March 1998; received in revised form 6 May 1998; accepted 13 July 1998

Abstract

Solid structures of the compositionally fractionated bacterial poly(3-hydroxybutyric acid-co-3-hydroxypropionic acid)s [P(3HB-co-3HP)], bearing much narrower comonomer compositional distributions, were studied by high-resolution solid-state ^{13}C n.m.r. $^{1}H-^{13}C$ cross-polarization relaxation behaviour (T_{CH} and $T_{1\rho}^{H}$) of chain-carbon nuclei was found to strongly depend on the micro-environments they were involved in, and the resonance contributions pertaining to different phases were therefore distinguished. Employing CP/MAS and PST/MAS methods, ^{13}C resonance signals from the crystalline and non-crystalline regions were selectively enhanced. The observed chemical shifts demonstrated that co-crystallization did not occur in the P(3HB-co-3HP) system. Spin-lattice relaxation times (T_1^C) of carbon nuclei attributed to 3HB and 3HP units were found to be considerably different, reflecting their distinguishable difference in local segmental dynamics. From the lineshape analyses of 3HB methyl carbon resonance measured by a DD/MAS method, it was revealed that the presence of minor 3HP comonomer units significantly suppressed the crystallization of a 3HB-rich semicrystalline copolyester. In addition, a correlation was found between average block length of 3HB sequences estimated by solution-state ^{13}C n.m.r. spectra and crystallizability of semi-crystalline copolyesters.

Keywords: P(3HB-co-3HP); Comonomer compositional distribution; Solid-state n.m.r.

1. Introduction

There are numerous reports on the study of poly(hydroxyalkanoic acid)s (PHA), a class of aliphatic polyesters naturally accumulated by a wide variety of environmental microorganisms, which are now of great importance due to their biodegradabilities and biocompatibilities [1–5]. The variation in carbon sources can produce large kinds of bacterial polyesters with diverse physical properties [4]. Further, physical characterization of the harvested bacterial polyesters have been extensively done by many investigators [6]. Besides, it is interesting that by adjusting the feeding ratio of carbon sources in complex media it is possible to develop several kinds of bacterial copolyesters with desirable physical properties [1,4]; for instance, the physical characteristics of the commercialized bacterial poly(3-hydroxybutyric acid-co-3-hydroxyvaleric acid) [P(3HB-co-3HV)] can be tailored by designating a desired 3HV comonomer content [7].

So far, it is well known that the physical properties of a given bacterial copolyester will, in principle, be regulated by such putative factors as comonomer structure, average comonomer composition, comonomer compositional distribution, etc. To date, the effects of the former two factors have been extensively investigated, while the third factor has, more or less, been neglected. In fact, the solvent/non-solvent fractionations of bacterial P(3HB-co-3HV)s by Mitomo et al. [8], [9] and Yoshie et al. [10] have demonstrated the presence of extremely broad comonomer compositional distributions. Hence, strictly, the apparent properties of a bacterial copolyester are statistically averaged values of those of copolyester chains bearing different comonomer compositions, thus resulting in an uncertainty in physical characterization. To exclusively clarify the comonomer composition dependence of physical properties for bacterial copolyesters, samples bearing no or narrower comonomer compositional distributions are indeed needed.

* Corresponding author.

0032-3861/99/$ - see front matter
PII: S0032-3861(98)00544-8

In a previous work [11], the copolyester poly(3-hydroxybutyric acid-co-3-hydroxypropionic acid)s

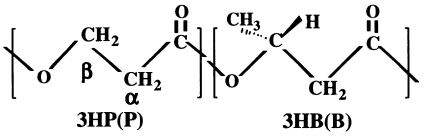

P(3HB-*co*-3HP)

biosynthesized by the bacterium strain *Alcaligenes latus* (ATTC 29713) have been fractionated via chloroform/*n*-heptane mixed solvent. The comonomer compositional distribution, thermal and crystallization behaviour have been thereby clarified for both 'original' as-produced P(3HB-co-3HP)s and their fractions. The evidences provided by solution ^{13}C n.m.r. analyses clearly indicated the much narrower comonomer compositional distributions of the fractionated copolyesters as compared to those of the original unfractionated bacterial products.

On the basis of the fractionated P(3HB-co-3HP)s bearing narrower comonomer compositional distributions, the primary objective of this paper is to examine the 3HP monomer-content dependence of solid structure by means of ^{13}C n.m.r. spectroscopy. Firstly, the dependence of magnetization transferring rate from naturally abundant ^{1}H to ^{13}C nuclei on either the sites of carbon atoms or phases in which they located, will be studied by CP/MAS (cross polarization/magic angle spinning) ^{13}C n.m.r. experiments with various contact times. Subsequently, utilizing CP/MAS and PST (pulse saturation)/MAS methods [12], the informative signals attributable to crystalline and amorphous origins are selectively enhanced. The possibility of occurrence of co-crystallization phenomenon in the P(3HB-co-3HP) copolyester system is critically discussed on the chemical shifts. Further, local dynamics will be studied by analysing the ^{13}C spin-lattice relaxation behaviour in the laboratory frame. The deconvolution of resonance lines acquired by DD (fully relaxed dipolar decoupling)/MAS method is performed to quantitatively study the detailed phase structure. Moreover, combining the results obtained from solution ^{13}C n.m.r. measurements, the correlation between microstructure and crystallizability of copolyester chain will be clarified.

2. Experimental

2.1. Materials

Bacterial P(3HB) purchased from Aldrich (Lot no. 00925KF) was purified with chloroform and *n*-hexane prior to use. P(3HP) chemically synthesized through ring-opening-polymerization of propiolactone was supplied by Tokuyama Corp. (Tsukuba, Japan) and in turn purified in the same way as for P(3HB). A series of P(3HB-co-3HP) samples with narrow comonomer compositional distributions were prepared via the chloroform/*n*-heptane fractionation of bacterial P(3HB-co-3HP)s as elucidated in a previous paper [11]. The characteristics of P(3HB), P(3HP) and the fractionated copolyesters with 3HP contents spanning the whole range of comonomer composition are summarized in Table 1.

2.2. Analytical procedures

High-resolution solid-state ^{13}C n.m.r. spectra were measured at ambient temperature on a JEOL GSX-270 spectrometer operating at 67.9 MHz. Each polymer sample was packed into a zirconia rotor with a polyimide cap. All n.m.r. spectra were recorded under high-power proton dipolar-decoupling (ca. 54.1 kHz) at the optimized MAS rate of 4.4–4.6 kHz, and 512–2048 free induction decays (FID) were accumulated with 2-k data points. In the common CP/MAS ^{13}C n.m.r. experiment, $^{1}H-^{13}C$ contact times (CT) were set to 2–4 ms, depending on different

Table 1
Characteristics of the fractionated P(3HB-co-3HP)s and homopolymers P(3HB) and P(3HP)[a]

Sample code	3HP (mol%)	M_n ($\times 10^{-5}$)	M_w/M_n	Remarks
P(3HB)	0	2.13	1.52	Bacterial origin
AF0	36.5	2.65	2.53	Original
AF9	13.2	1.76	1.86	Fractionated
AF8	15.9	2.57	2.34	Fractionated
AF7	23.8	2.40	2.51	Fractionated
AF6	21.9	2.03	2.90	Fractionated
AF5	38.3	2.17	2.97	Fractionated
AF4	48.0	1.65	3.43	Fractionated
AF3	53.1	3.09	1.90	Fractionated
AF2	60.1	3.33	2.12	Fractionated
AF1	73.6	4.49	1.76	Fractionated
BF4	77.9	1.87	3.08	Fractionated
BF3	86.2	2.45	1.45	Fractionated
BF2	89.6	1.83	2.22	Fractionated
BF1	95.9	2.50	1.76	Fractionated
P(3HP)	100	1.54	2.32	Chemosynthetic

[a]Details in Ref. [11].

crystallinities of the investigated polymers. Similarly, the pulse-saturation times of PST/MAS method were optimized from 20 to 30 s in accordance with the local dynamics of copolyesters in the amorphous regions. Conventional CPT1 pulse sequence developed by Torchia [13] was applied to monitor the spin-lattice relaxation behaviour of the semi-crystalline polymers, and ^{13}C spin-lattice relaxation times (T_1^C) were approximately estimated by the so-called empirical bi-exponential model [14]. A pulse repetition time of 5 s was used in both CP/MAS and PST/MAS ^{13}C n.m.r. experiments. It is necessary that a repetition time should be longer than at least five times relaxation time (T_1^C) of an interested carbon nucleus for ensuring the complete recovery of the equilibrium magnetization [15]. Hence, for acquiring accurately the signals attributed to different phases in the DD/MAS experiment, a repetition time was practically set to 30 s which was confirmed to be longer than five times T_1^C of methyl carbon of the 3HB unit in the crystalline region. ^{13}C n.m.r. chemical shifts were referred to the CH_3 resonance of hexamethylbenzene, which was used as the external standard (17.4 ppm from TMS).

To estimate the average block length of 3HB sequences of the fractionated copolyesters, ^{13}C solution n.m.r. spectra in $CDCl_3$ were measured at room temperature on a JEOL GSX-270 spectrometer operating at 67.9 MHz, with 8.2 μs pulse width (90° pulse), 27027 Hz spectra width, 64-k data points, 5 s repetition time and 16 000–20 000 FID accumulations.

Lineshape analyses of the interested carbon resonances were performed as follows: firstly, the original FID real data were zero-filled to 8-k, then Fourier-transformed and phase corrected. Subsequently, the deconvolution of resonance line was carried out by the least squares method on an assumption of the Lorentzian lineshape mathematically described as

$$L(x) = \frac{Y_0 W^2}{W^2 + 4(x - x_0)^2} \quad (1)$$

where Y_0, W and x_0 express the maximum height, the half-height width, and the centre of the deconvoluted peak, respectively. The contributions combined to reproduce the original resonance lines were assignable to the resonances stemming from the carbon nuclei locating in different molecular environments. Consequently, the dependence of crystallization behaviour on comonomer content was quantitatively discussed in detail.

3. Results and discussion

3.1. CP/MAS ^{13}C n.m.r. spectra and cross-polarization relaxation behaviour

Fig. 1 depicts the integrated ^{13}C resonance intensities for P(3HB) as a function of CP contact time (t). The resonance intensity of carbon at each site of 3HB unit initially

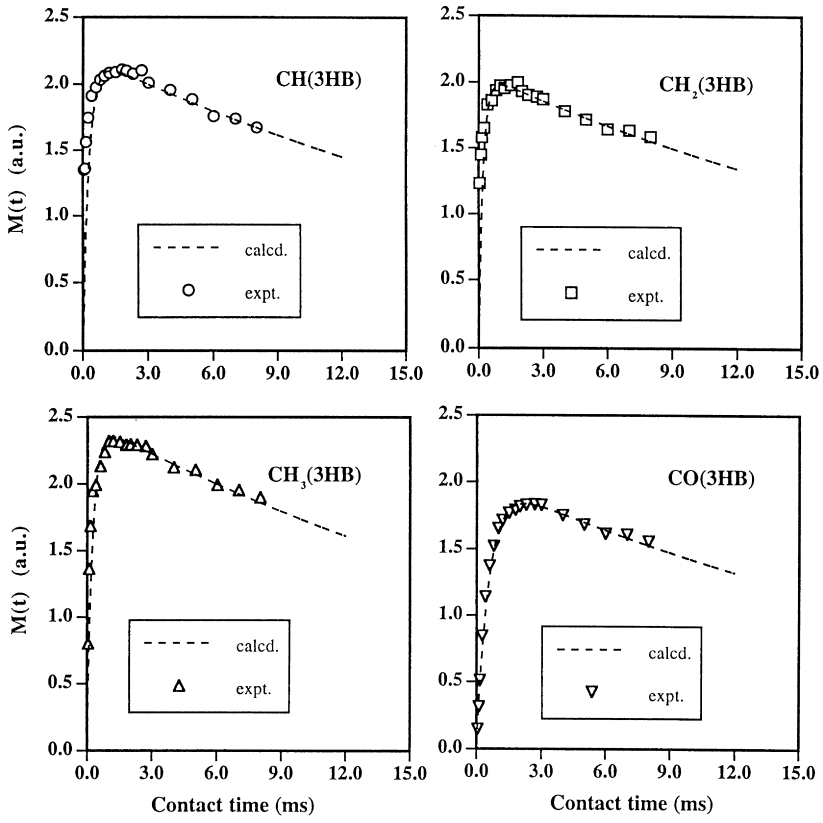

Fig. 1. The integrated resonance intensities of carbon nuclei at different sites as a function of contact time for P(3HB). (Dashed line: calculated by the curve-fittings according to Eq. (2)).

increases rapidly, and finally decreases in a more gradual manner. In principle, under the matched Hartmann-Hahn condition, ^{1}H and ^{13}C magnetizations locked in their individual channels are mixed, and magnetizations of naturally abundant protons will transfer to those of rare ^{13}C nuclei through the short-range static $^{1}H-^{13}C$ dipolar interaction [16]. According to the cross-polarization dynamics [17], ^{13}C magnetization buildup can be mathematically expressed by invoking cross-polarization relaxation time (T_{CH}) and proton spin-lattice relaxation time in the rotating frame ($T_{1\rho}^{H}$) as follows,

$$M_c(t) = M_0 \frac{T_{1\rho}^{H}}{T_{1\rho}^{H} - T_{CH}} \left(e^{1/T_{1\rho}^{H}} - e^{t/T_{CH}} \right) \quad (2)$$

where M_0 is a constant for each carbon at the specific site. In Fig. 1, the fitting results shown as dash lines are also presented. Here, it should be noted that the integrated intensities are apparent values, involving contributions ascribed to the resonances in different phase structures. Fortunately, due to the high crystallinity of P(3HB) as reported to be about 60–80% [1,2], the integrated intensities can be thought as mainly reflecting the resonance in the crystalline portion, because of higher CP efficiencies of carbon nuclei in the crystalline regions than those in the amorphous regions [18]. T_{CH} values estimated by the curve-fittings are summarized in Table 2. The proton-bonded carbon nuclei exhibited shorter cross-polarization relaxation times than carbonyl carbon, indicating their faster magnetization transferring rates due to the static interactions through $^{1}H-^{13}C$ dipolar coupling.

In a view of Table 2, $T_{1\rho}^{H}$ values of 28.0 ms obtained by curve-fittings seem to be independent of the specific site in the 3HB unit. This phenomenon can be accounted for by the efficient spin diffusion over the proton ensembles in the crystalline regions [19]. In Table 2, CP relaxation behaviour for P(3HP) are also described. In contrast to P(3HB), carbon nuclei at the corresponding sites of P(3HP) show relatively shorter T_{CH} values, indicating their faster cross-polarization relaxation behaviour.

Recently, Du Prez et al. [20] reported that the CP experiments combined with MAS were capable of distinguishing the multiple phases in poly(1,3-dioxolane). Accordingly, the variable-contact time CP/MAS ^{13}C n.m.r. experiments were done for the fractionated P(3HB-co-3HP)s. Fig. 2 enumerates the resonance of methylene carbon at the α-site of 3HP unit (situating around 31.0–34.0 ppm) as a function of contact time for P(3HB-co-86.2 mol%3HP), interestingly indicating the splitting of resonance signals. The split situating at 34.2 ppm appears later and is assignable to the resonance arisen from the nuclei in the amorphous regions due to its slower magnetization transferring rate. Thus, it can be concluded that 3HP units were distributed in at least two phase structures. The results of X-ray diffraction [11] revealed that the fractionated 3HB-rich and 3HP-rich copolyesters were semi-crystalline polymers, forming 2_1 helix crystalline structures having lattice parameters corresponding to those of P(3HB) and P(3HP), respectively. The evidences provided by the variable-contact time ^{13}C n.m.r. experiments confirm that the 3HP units are essential to comprise the P(3HP) lattice-type crystallites for the 3HP-rich semi-crystalline copolyesters. Furthermore, these interested carbon resonances were deconvoluted into two contributions situating at 34.2 and 31.3 ppm, which, respectively, represent the resonances in the amorphous and crystalline regions. Results of curve-fittings are presented in Table 2. The T_{CH} value for the nuclei in the amorphous regions is longer than that in the crystalline regions, suggesting faster molecular motion in the amorphous regions.

In general, maximum resonance intensities were observed at a contact time of around 1.8–2.5 ms for different nuclei of homopolymers and the fractionated copolyesters. Therefore, a contact time of 2.0 ms was applied as the common condition in the following CP/MAS ^{13}C n.m.r. experiments.

3.2. Chemical shift and phase structure

Isomorphism, a phenomenon of co-crystallization observed in the bacterial P(3HB-co-3HV) system, has extensively been studied by many investigators [21–25]. We here focus our attentions on the study whether the same phenomenon occurs in the bacterial P(3HB-co-3HP)s.

Table 2
Cross-polarization relaxation times T_{CH} and proton spin-lattice relaxation times in the rotating frame $T_{1\rho}^{H}$ for P(3HB), P(3HP) and P(3HB-co-86.2 mol%3HP)

Sample	CH(3HB)		CH_2(3HB)		C=O		CH_2(3HP-β)		CH_2(3HP-α)			
	T_{CH}	$T_{1\rho}^{H}$	T_{CH}	$T_{1\rho}^{H}$	T_{CH}	$T_{1\rho}^{H}$	T_{CH}	$T_{1\rho}^{H}$	T_{CH}(c)[d]	$T_{1\rho}^{H}$(c)[d]	T_{CH}(a)[d]	$T_{1\rho}^{H}$(a)[d]
P(3HB)[a]	0.28	28.0	0.20	0.25	28.0	0.56	28.0					
P(3HB-co-86.2 mol%3HP)[b]									0.24	14.5	0.56	10.0
P(3HP)[c]						0.50	14.0	0.15	14.0	0.16	14.0	

[a,c]Indicate the results obtained by fitting the total carbon resonance intensities at the individual sites according to Eq. (2).

[b]Expresses the values derived from fitting α-carbon resonance intensities attributed to the crystalline and amorphous phases with the aid of resonance line deconvolution.

[d]T_{CH}(c), $T_{1\rho}^{H}$(c), T_{CH}(a) and $T_{1\rho}^{H}$(a) represent the relaxation times in the crystalline and amorphous regions.

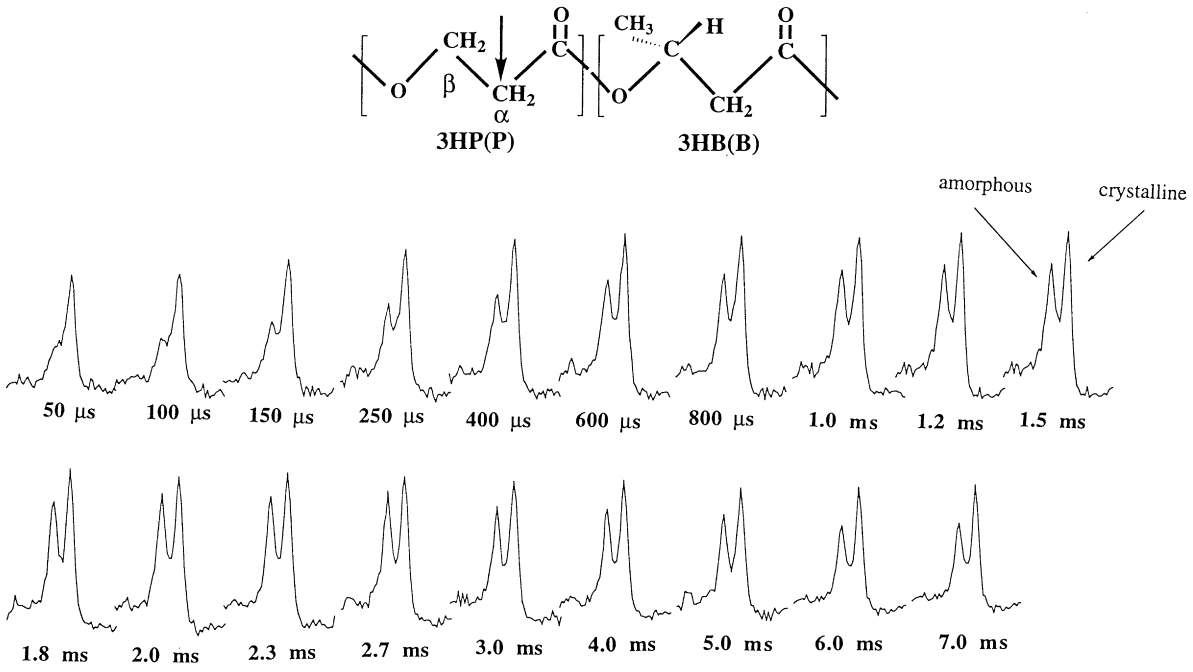

Fig. 2. The ^{13}C n.m.r. resonance line of CH_2 at the α site of 3HP unit for P(3HB-co-86.2 mol% 3HP) as a function of CP contact time.

Chain carbons included in the individual molecular environments (e.g. the ordered crystalline, disordered and transitional regions, etc.) are known to exhibit the different chemical shifts and relaxation behaviour for semi-crystalline polymers [15], [23], [24]. In this study, ^{13}C n.m.r. spectra were measured by CP/MAS and PST/MAS methods for the purpose to preferentially acquire the signals attributable to the crystalline and amorphous regions, respectively.

Fig. 3 depicts the CP/MAS ^{13}C n.m.r. spectra of homopolymers and the fractionated copolyesters with various 3HP contents. Resonance features can be approximately divided into two groups, i.e. the copolyesters with 3HB-rich comonomer (13.2–48.0 mol% 3HP) show spectra quite similar to the spectrum of P(3HB), whereas the P(3HP)-type resonance features are observed for the 3HP-rich copolyesters. Further, in the order of increasing 3HP content, the broadening of resonance is explicitly detected, particularly for the 3HB methyl carbon resonance. Even though the accumulation time was increased from 512 for P(3HB) to 2048 for P(3HB-co-48.0 mol%3HP), only a spectrum with poor *S/N* ratio could be obtained for the latter due to the significantly lowered crystallinity. In addition, it is noted that the intensities of signals attributed to the 3HP units are found to be close to noise level despite the variation of 3HP content (13.2–48.0 mol% 3HP). This may be resulted from the poor CP efficiencies because the 3HP units are entirely excluded into the amorphous regions. On the

Table 3
Solid-state ^{13}C chemical shifts of chain carbons at the different sites for the fractionated P(3HB-co-3HP)s, P(3HB) and P(3HP)[a]

Sample code	C=O		CH(B)		CH_2(P-β)		CH_2(B)		CH_2(P-α)		CH_3(B)	
	CP	PST	CP	PST	CP	PST	CP	PST	CP	PST	CP	PST
P(3HB)	169.6	169.9	68.5	68.5	—	—	42.9	42.9	—	—	21.3	21.3
AF9(13.2)	169.8	169.8	68.5	68.5	61.4	n.d.[b]	42.8	42.7	35.2	n.d.	21.3	21.3
AF7(23.8)	169.6	170.0	68.4	68.4	61.5	61.5	42.7	42.7	35.4	35.4	21.3	21.3
AF5(38.3)	170.0	170.6	68.6	68.4	n.d.	61.1	42.9	41.5	n.d.	34.5	21.3	20.1
AF4(48.0)	170.2	170.5	68.7	68.1	n.d.	60.7	42.8	40.8	n.d.	34.3	21.3	20.1
AF2(60.1)	170.6	170.9	68.7	68.5	61.3	61.1	41.1	41.1	34.7	34.2	20.1	20.1
BF4(77.9)	172.9	171.2	68.5	68.5	62.2	61.1	41.3	41.3	34.1,31.1	34.1	20.1	20.1
BF3(86.2)	172.9	171.0	68.1	68.4	61.9	60.8	41.3	41.3	34.1,31.1	34.1	20.1	20.1
BF2(89.6)	172.8	171.1	n.d.	68.3	62.2	61.0	n.d.	41.2	31.0	34.2	20.1	20.1
BF1(95.9)	172.9	171.1	n.d.	n.d.	61.9	61.0	n.d.	n.d.	31.0	34.1,31.2	n.d.	20.1
P(3HP)	172.9	171.1	—	—	62.0	61.6	—	—	31.0	34.1,31.3	—	—

[a]Chemical shift in ppm from TMS.
[b]Not detected.

other hand, the 3HP-rich copolyesters (77.9–95.9 mol% 3HP) show similar resonance features to that of P(3HP). The CH_2(3HP-α) resonance contribution at 34.2 ppm attributable to the amorphous regions can be visualized when the 3HP unit content decreases from 100 mol% [P(3HP)] to 77.9 mol% [P(3HB-co-77.9 mol%3HP)].

Fig. 4 shows the PST/MAS ^{13}C n.m.r. spectra of homopolymers and copolyesters for acquiring the signals attributable to the amorphous component. During the experiments, pulse saturation time was practically optimized from 20 to 30 ms for the samples with decreasing 3HP content. The strongest resonance intensities are observed for the 3HB methyl carbons. Since the 3HB methyl group is highly mobile, its resonance is significantly enhanced by the so-called heteronuclear NOE during the pulse saturation process.

In order to make clear the dependence of the ^{13}C resonance line on the phase structure, chemical shifts obtained from the CP/MAS and PST/MAS spectra are summarized in Table 3. The ^{13}C resonances of CH_3(3HB) and CH_2(3HP-α) are chosen to analyse the effect of solid structure on ^{13}C chemical shift. For the 3HB methyl carbon, only resonance contributions situating at about 20.1 ppm attributed to the amorphous regions are detected for the 3HP-rich copolyesters (AF2–BF1). In contrast, for the 3HB-rich copolyesters (AF9–AF4), the contributions ascribed to the resonances in the amorphous regions are obscured by the stronger resonances at 21.3 ppm assignable to the crystalline

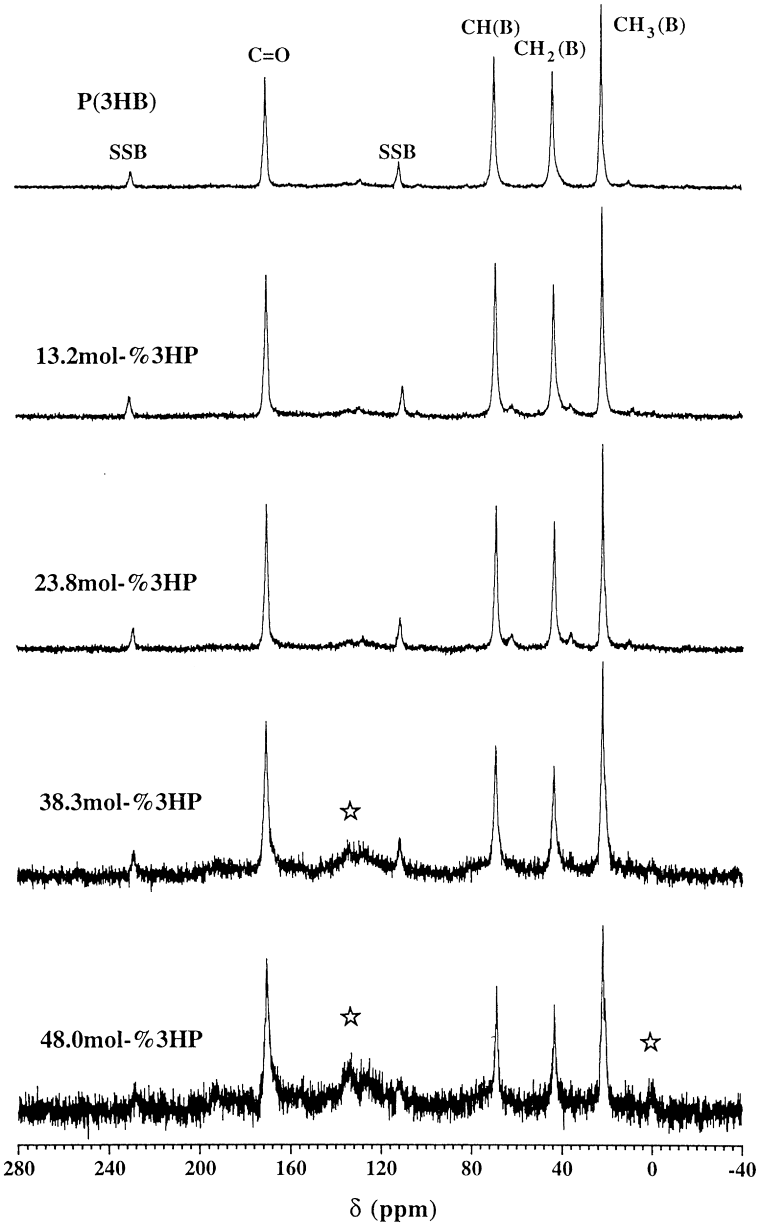

Fig. 3. The 67.9 MHz ^{13}C CP/MAS n.m.r. spectra of P(3HB-co-3HP)s, P(3HB) and P(3HP). The broad resonances indicated by ☆ arose from the n.m.r. rotor; the peaks marked by SSB indicate the spinning side bands.

regions. Therefore, it can conclude that the 3HB units are excluded from the P(3HP)-type crystalline structures of semi-crystalline 3HP-rich copolyesters. Similarly, inspecting the chemical shifts of methylene carbon resonances at the α site of 3HP unit, only signals at 34–35 ppm are detected for the 3HB-rich copolyesters (AF9–AF2) regardless of the variation of observation pulse. However, the appearances of contributions at about 31 ppm assignable to the crystalline regions as mentioned, are observed for the 3HP-rich semicrystalline copolyesters, which formed the P(3HP)-type lattice structures. Therefore, it can be revealed that the 3HP units are excluded from the P(3HB)-type crystallites of the 3HB-rich semicrystalline copolyesters. Hence, combining the above-mentioned two conclusions, we can demonstrate that the co-crystallization phenomenon does not occur in this P(3HB-co-3HP) copolyester system. Here, it is worthwhile pointing out that the multiple endothermic peaks in the d.s.c. traces of the unfractionated bacterial copolyesters [11] likely lead to a misunderstanding of co-crystallization. In fact, this accounts for the presence of extremely broad comonomer compositional distributions as reported [8–10], [26–28].

3.3. ^{13}C spin-lattice relaxation time T_1^C and local motion

To clarify the possible cause of the experimental fact that the 3HB and 3HP units cannot co-crystallize in the semi-crystalline P(3HB-co-3HP)s. ^{13}C spin-lattice relaxation times, T_1^C, were measured by the conventional CPT1 pulse sequences [13], and their local dynamics were analysed. In a

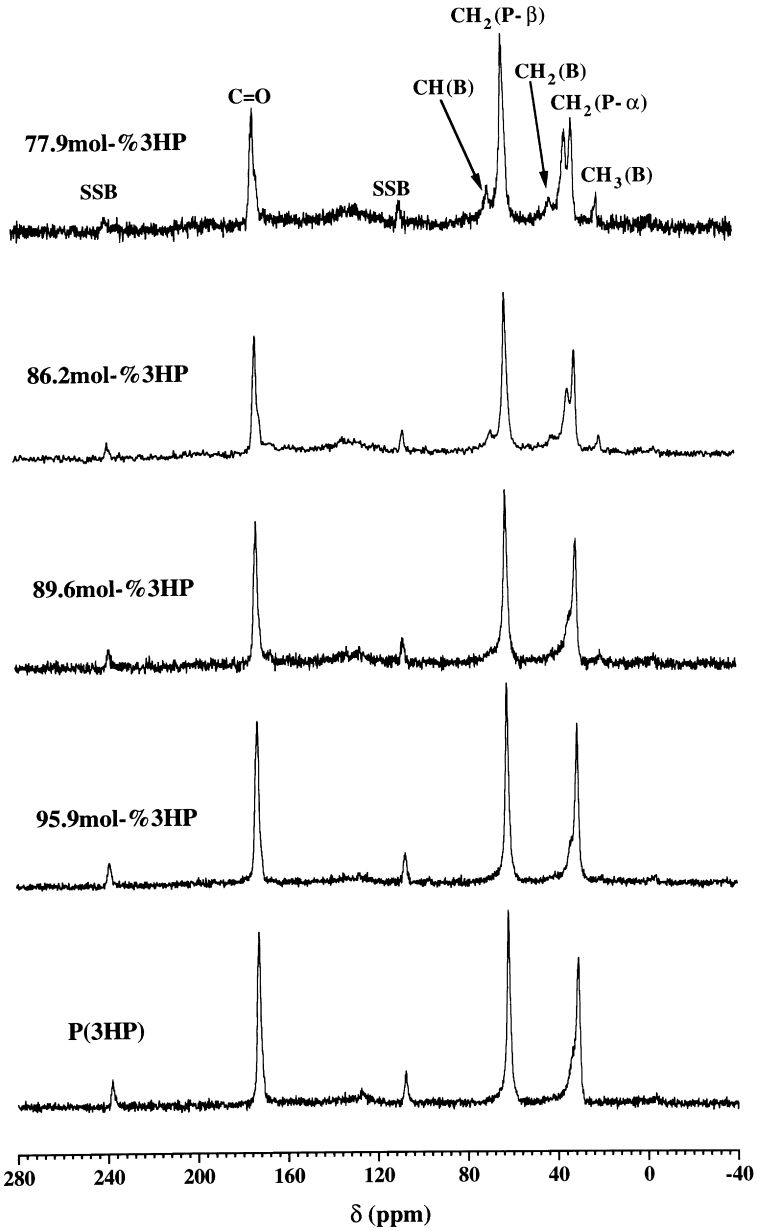

Fig. 3. Continued.

more recent report [14], the longitudinal relaxation behaviour was revealed for the 3HB-rich semicrystalline P(3HB-co-3HP)s. The present work is devoted to the investigation of the 3HP-rich semicrystalline copolyesters, which form the P(3HP)-type crystal structures.

Table 4 presents the T_1^C values of different carbons for the 3HB and 3HP units, which were estimated according to the two-component relaxation model based on Eq. (3)

$$M(t) = M_{a0} \exp\left(-\frac{t}{T_{1a}^c}\right) + M_{c0} \exp\left(-\frac{t}{T_{1c}^c}\right) \quad (3)$$

where M_{a0} and M_{c0} are the initial ^{13}C magnetizations in the amorphous and crystalline regions, and T_{1a}^C and T_{1c}^C are the corresponding relaxation times. As seen in Table 4, the T_{1a}^C values with an order of second are associated with the fast motion occurring in the amorphous regions, while the longer T_{1c}^C values are reasonably ascribed to the restricted local motion in the well-ordered crystalline regions. Spyros and co-workers [29–31] reported a higher temperature of around 80°C, at which the minimum T_{1a}^C value was observed in the T_{1a}^C versus $1/T$ plot (T, absolute temperature) for the backbone carbons of P(3HB). This suggests that the local motion of P(3HB) backbone carbons in the amorphous regions locates in the regime of slow motion ($\omega^2\tau_c^2 > 1.0$; here, ω and τ_c are the resonance frequency and the correlation time, respectively) at room temperature. Strictly, it is difficult to compare the local motion of different comonomer units in copolyesters without the measurements of T_{1a}^C values at wide-range temperatures and at different

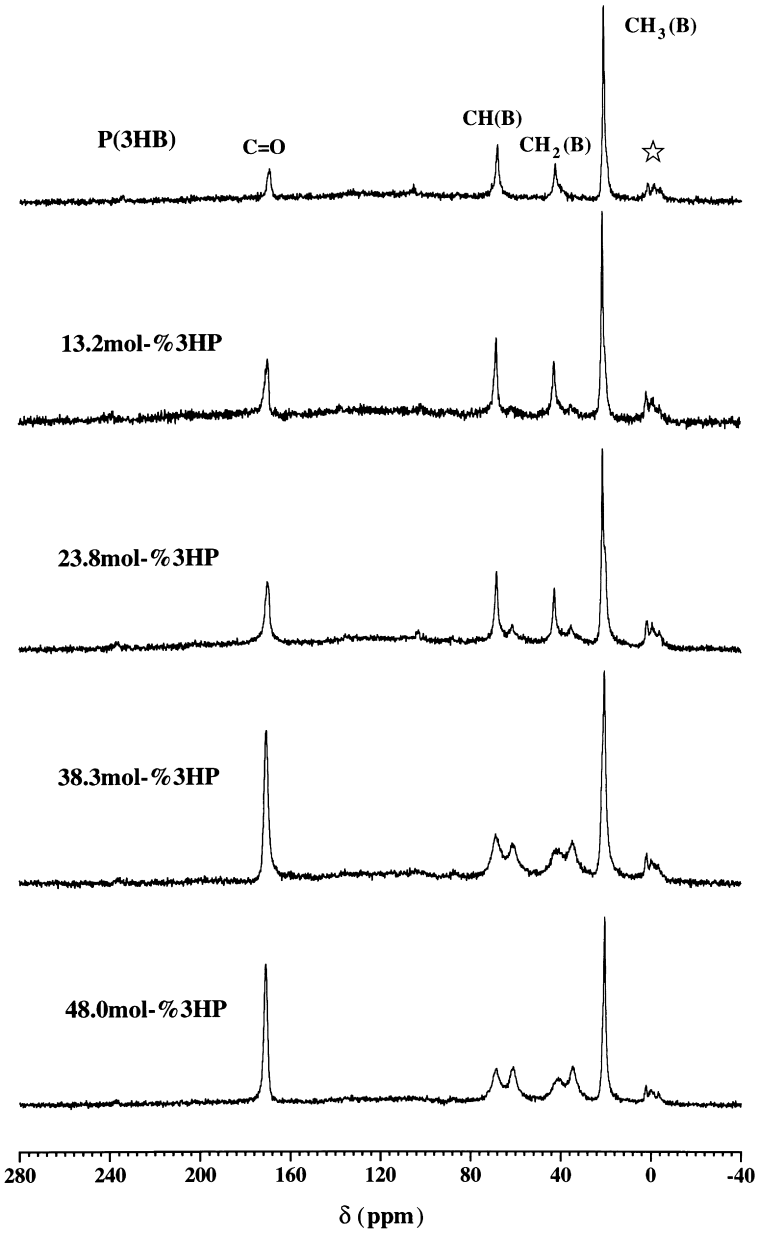

Fig. 4. The 67.9 MHz ^{13}C PST/MAS n.m.r. spectra of P(3HB-co-3HP)s, P(3HB) and P(3HP). The resonances indicated by ☆ arose from the n.m.r. rotor.

static magnetic fields. However, the comparison of T_{1a}^{C} values of carbon nuclei at the fixed sites in the same comonomer units can be made to clarify the influences from the presence of the second comonomer units. As seen from Table 4, the T_{1a}^{C} value of carbon atom at either the α or β site of the 3HP unit monotonously increases with the increase in the 3HP content for the 3HP-rich semicrystalline copolyesters. Since the glass transition temperatures of these copolyesters were revealed to linearly decrease with the increase in the 3HP content, increased chain mobility is implied [11]. Therefore, the results of T_{1a}^{C} and glass transition temperature suggest that the local motion of the 3HP backbone carbons in the amorphous regions falls in the regime of fast motion at ambient temperature. In addition, the T_{1a}^{C} values of carbon atoms at the same site of 3HB and 3HP units seem to be considerably different at room temperature, indicating their distinguishable difference in local dynamics.

3.4. Lineshape analysis and the partitioning of 3HB units in different phases

It is well known that lineshape analyses for fully relaxed DD/MAS ^{13}C n.m.r. spectra are very useful for elucidating the detailed phase structure of different polymers [24,32]. In this study, the methyl carbon resonance of the 3HB unit was quantitatively analysed. To measure the fully relaxed spectrum for the methyl carbon, the pulse repetition time was

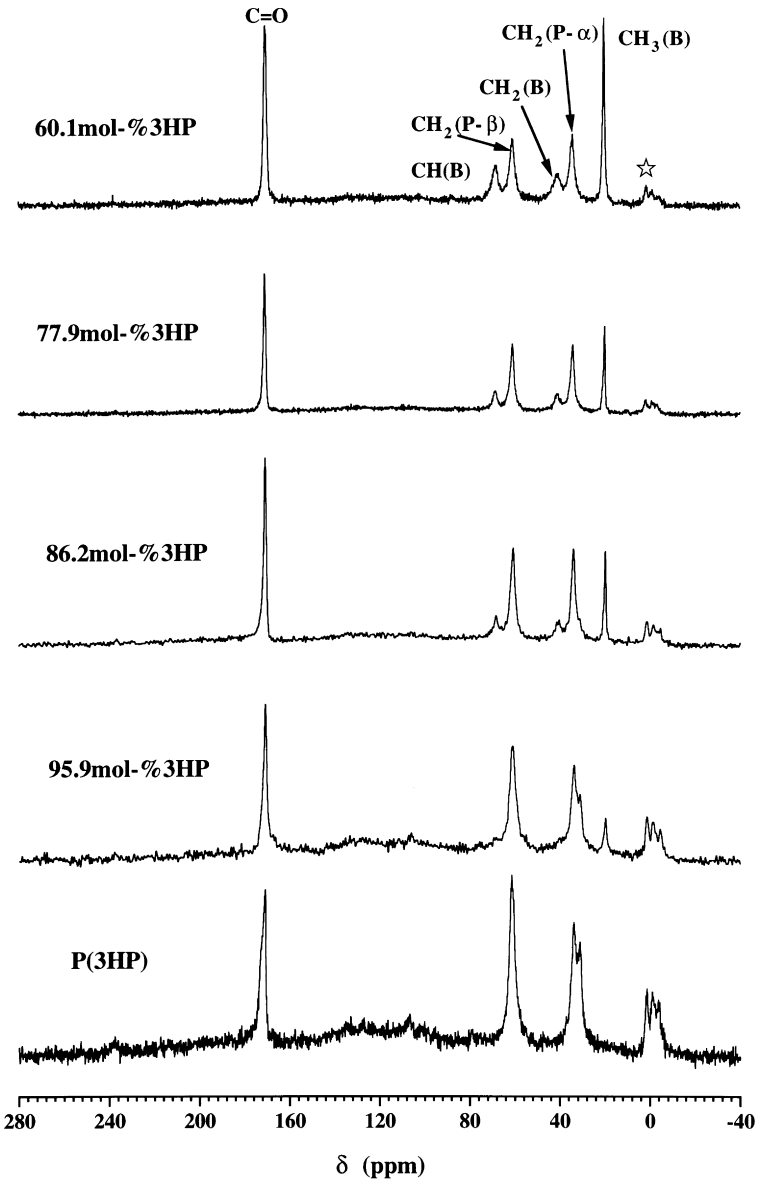

Fig. 4. Continued.

adjusted to 30.0 s, which was greater than five times T_1^C in the crystalline regions.

Fig. 5 depicts the DD/MAS spectra of the copolyesters and P(3HB). The methyl resonance is obviously broadened with the increase in 3HP unit content. The shoulder observed on the upfield side for the methyl resonance is assigned to the amorphous component, as already described above. Fig. 6 shows the deconvolution results of methyl carbon resonances on an assumption of Lorentzian lineshape. Here, components 1 and 2 at 20.1 and 21.3 ppm with linewidths of ca. 103 and 51 Hz are assignable to the resonances in the amorphous and crystalline regions, respectively. Due to the asymmetrical features of methyl carbon resonances, as shown in Fig. 6, a third component (3), as a shoulder at 22.2 ppm with a linewidth of ca. 61 Hz, is practically extracted. As seen in Fig. 6, the contribution of the crystalline component, 2, expressed as the area percentage of methyl carbon resonance, decreases with the increase in the 3HP content, indicating a significant suppressing effect of the 3HP unit on the crystallization of the 3HB-rich copolyesters. In contrast to components 1 and 2, less change in relative intensity of component 3 is observed despite the variation in the 3HP content. Schaefer et al. [16] reported that the broadening of ^{13}C n.m.r. resonance was caused by the conformational change and chain-orientation in some solid glassy polymers. Most recently, a third component with mass fraction of 0.41, which is assignable to the interfacial

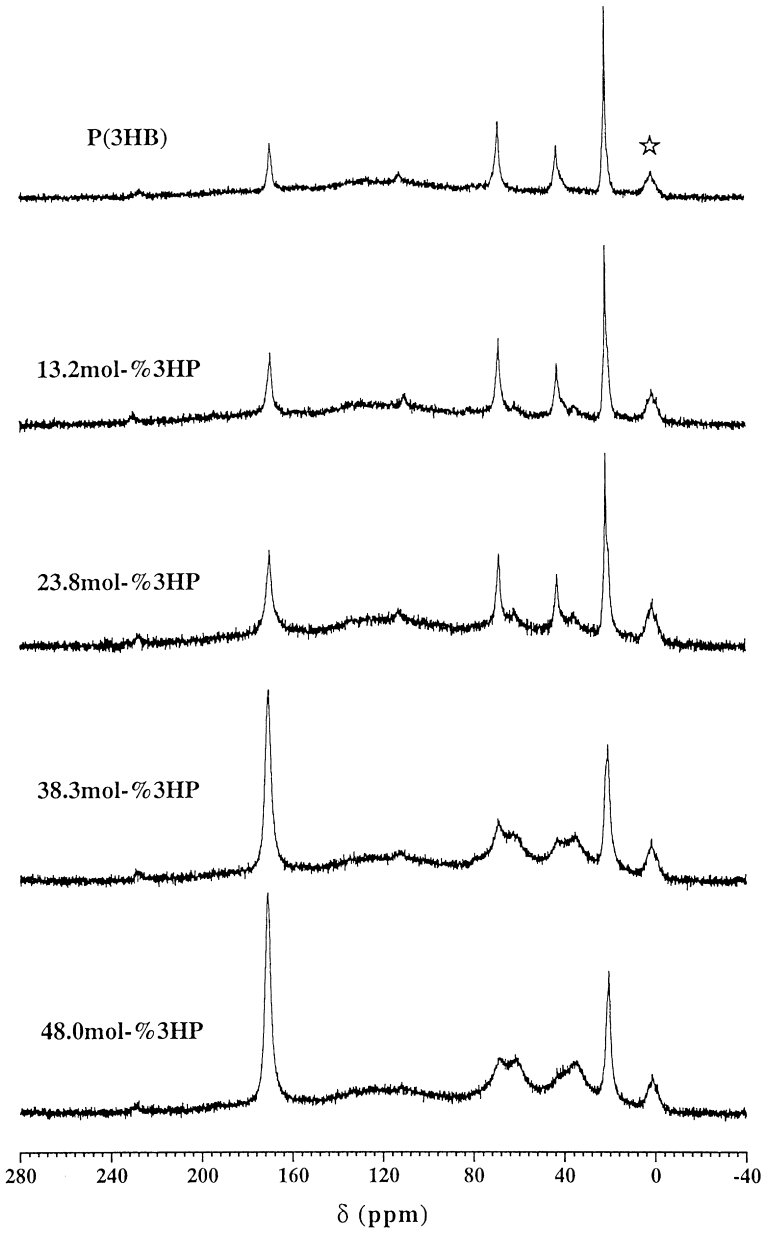

Fig. 5. The 67.9 MHz ^{13}C DD/MAS n.m.r. spectra of a series of 3HB-rich P(3HB-co-3HP)s as well as P(3HB). The resonances indicated by ☆ arose from the n.m.r. rotor.

regions for linear low-density polyethylene, has been characterized by Kuwabara et al. [32] via a solid-state ^{13}C n.m.r. technique. In view of the resonance features, such as the linewidth and relative intensity for component 3, it may be assumed to be the contribution from the interfacial regions. However, a direct evidence should be needed.

3.5. Crystallizability and average block length of 3HB sequences

To clarify the crystallizability of the fractionated copolyesters, mass fractions χ_B and χ_P of the 3HB and 3HP units in their respective crystalline regions were estimated from the heat of fusion ΔH_m based on the d.s.c. traces (details in Ref. [11]) according to the following equations

$$\chi_B = \frac{\Delta H_m}{w_B} \cdot \frac{\chi_B^0}{\Delta H_B^0} \quad (4)$$

$$\chi_P = \frac{\Delta H_m}{w_P} \cdot \frac{\chi_P^0}{\Delta H_P^0} \quad (5)$$

where

$$w_B = \frac{86(1-x_P)}{86(1-x_P)+72x_P} \text{ and } w_P = 1 - w_B$$

in which x_P, w_B, w_P express the molar content of the 3HP unit and the weight fractions of the 3HB and the 3HP units in a copolyester, respectively; ΔH_m, ΔH_B^0 and ΔH_P^0 indicate the heat of fusion of a copolyester, P(3HB) and P(3HP), respectively [11]; χ_B^0 and χ_P^0 mean the degree crystallinities of P(3HB) and P(3HP) in the equilibrium crystallization state (see Ref. [11]); The values of 86 and 72 are the molar masses of the 3HB and the 3HP units, respectively. The results are depicted in Fig. 7. It is seen that the increase in the molar content of the secondary comonomer (minor component) gives rise to an obviously retarding effect on crystallizability of either a 3HB-rich (0–50 mol% 3HP) or a 3HP-rich (75–100 mol% 3HP) semicrystalline copolyester. The suppressing effect of a 3HB unit on the crystallization of the 3HP-rich copolyester is more prominent.

Hocking and Marchessault [33] reported that the average block length of (*R*–*S*)P(3HB)s could be related to the formation of single crystals and their degradation behaviour.

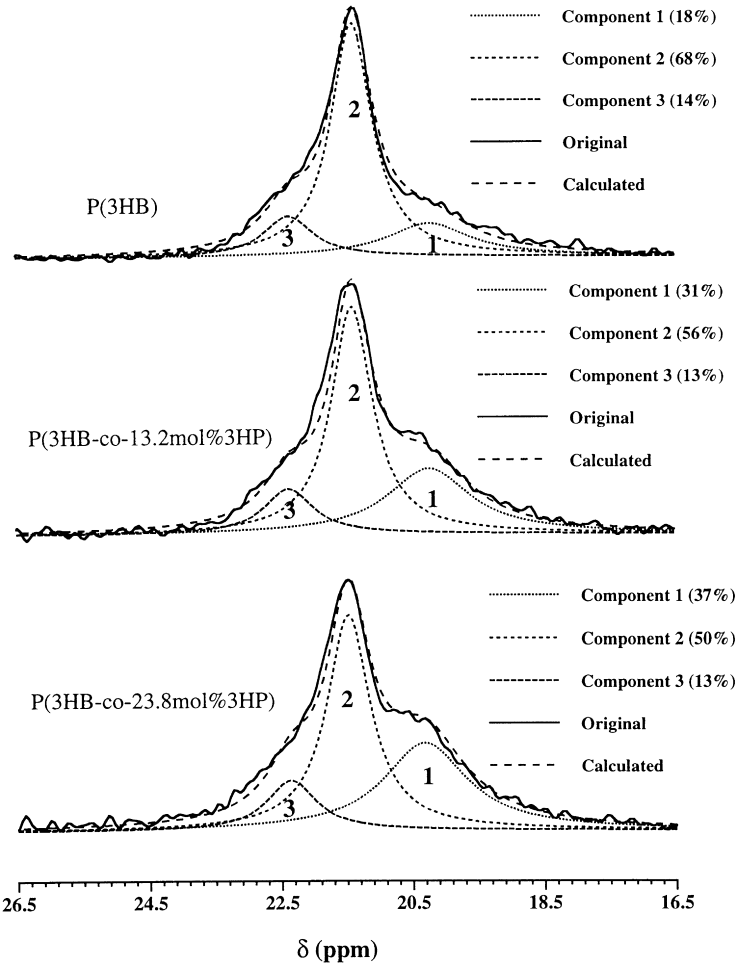

Fig. 6. Lineshape analyses of the 3HB methyl carbon resonances recorded by a DD/MAS method for P(3HB), P(3HB-co-13.2 mol%3HP) and P(3HB-co-23.8 mol%3HP). The values in parentheses indicate their relative resonance intensities calculated from area percentages.

Table 4
Solid-state ^{13}C spin-lattice relaxation times T_1^c (in seconds) of chain carbons at the different sites for the 3HP-rich P(3HB-co-3HP)s, P(3HB) and P(3HP)

Sample code	C=O		CH(B)		CH_2(P-β)		CH_2(B)		CH_2(P-α)		CH_3(B)	
	Fast	Slow	Fast	Slow	Fast	Slow	Fast	Slow	Fast	Slow	Fast	Slow
P(3HB)	56.5	85.5	9.9	79.4	—	—	4.8	72.1	—	—	0.7	2.2
BF4(77.9)	n.d.[a]	59.0			0.4	83.3			0.3	58.8		
BF3(86.2)	n.d.	87.0			0.6	90.9			0.5	76.9		
BF2(89.6)	n.d.	104.9			0.9	100.0			0.5	83.3		
BF1(95.9)	n.d.	138.8			0.9	125.0			0.7	125.0		
P(3HP)	9.2	72.7	—	—	1.0	76.9	—	—	1.0	83.3	—	—

[a]Not detected.

Here, we will shed new light on the parallelism between the crystallizability and the average block length of 3HB sequences for the P(3HB-co-3HP) copolyesters. Fig. 8 depicts the amplified methine carbon resonances recorded in solution for P(3HB) and P(3HB-co-53.1 mol%3HP), in which the well-resolved resonances can be assigned to the triad sequences [11,34]. Average block lengths of 3HB sequences were estimated according to Eq. (6) based on the model commonly used for a binary copolyer [35],

$$L_B(\text{exp.}) = \frac{I_{B\cdot B\cdot B} + I_{B\cdot B\cdot P}}{I_{P\cdot B\cdot B} + I_{P\cdot B\cdot P}} + 1 \quad (6)$$

where L_B(exp.) means the experimental average length of 3HB sequences, $I_{B\cdot B\cdot B}$, $I_{B\cdot B\cdot P}$, $I_{P\cdot B\cdot B}$ and $I_{P\cdot B\cdot P}$ express the individual triad integrated intensities. In Table 5, the average block lengths of the 3HB sequences are summarized along with the calculated values L_B(calcd.) on an assumption that the 3HB and 3HP units are randomly distributed [36],

$$L_B(\text{calcd.}) = \frac{1}{1 - x_B} \quad (7)$$

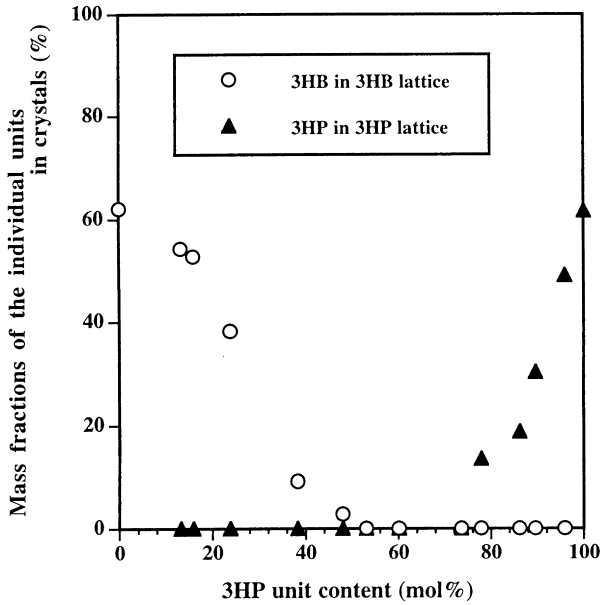

Fig. 7. The 3HP unit content dependence of mass fractions of the individual monomer units in the crystallites for different copolyesters.

where x_B represents the 3HB molar content of an investigated copolyester. As seen in Table 5 and Fig. 9, the decrease in the 3HB unit content leads to the marked decrease in the experimental average length of 3HB sequences, particularly for the copolyesters with the 3HB-rich comonomer. The fractionated copolyester P(3HB-co-48.0 mol% 3HP) with an average 3HB block length close to 2.0 exhibits χ_B close to 0, indicating a feature similar to the amorphous state. Here, it is noted that the average block length of 3HB sequences estimated by solution ^{13}C n.m.r. is the statistically averaged value for the all copolyester chains involved in a copolyester sample. The experimental results of L_B(exp.) and χ_B indicate that the copolyesters with L_B(exp.) longer than two 3HB units can form the P(3HB)-type crystal structures. The average block lengths of 3HP sequences L_P(exp.) for the 3HP-rich semicrystalline copolyesters were not investigated. However, the tendency as

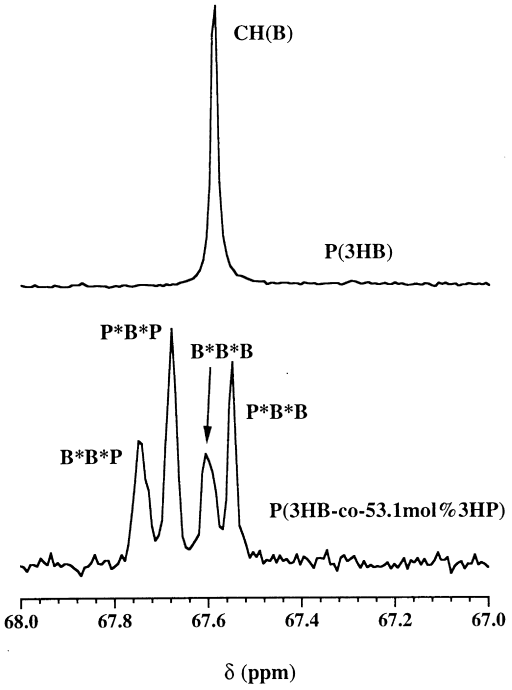

Fig. 8. The 67.9 MHz ^{13}C n.m.r. resonance of methine carbon for P(3HB) and P(3HB-co-53.1 mol%3HP) in $CDCl_3$ solution recorded at room temperature.

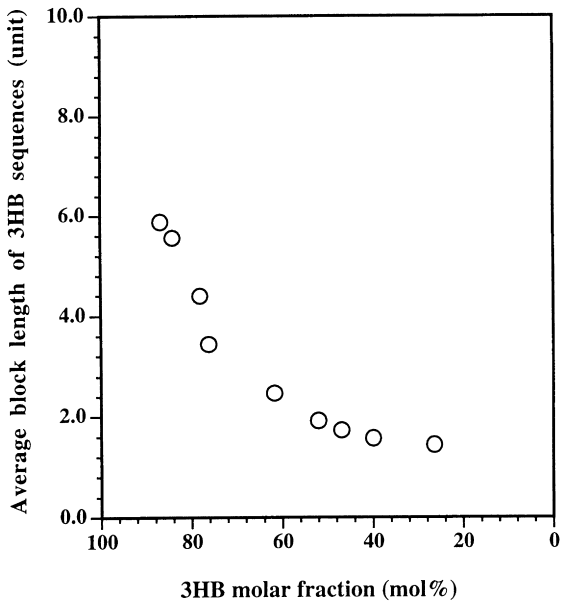

Fig. 9. The 3HB unit content dependence of the experimental average block length of 3HB sequences for the fractionated P(3HB-co-3HP)s.

seen in Fig. 7 indicates a more severe suppressing effect of the 3HB unit on the crystallizibility of the 3HP-rich semicrystalline copolyesters. This can be accounted for the fact that the amorphous 3HB units with pendant chains are more difficult to diffuse away from the 3HP crystallization front than the amorphous 3HP units in the cases of the 3HB-rich semicrystalline copolyesters.

4. Conclusion

In this paper, the solid structures of P(3HB) and P(3HP), as well as the fractionated bacterial P(3HB-co-3HP)s, bearing much narrower comonomer compositional distributions, were characterized by high-resolution solid-state ^{13}C n.m.r. The results can be summarized as follows:

(1) the $^{1}H-^{13}C$ cross-polarization relaxation behaviour was found to strongly depend on the solid structure. The CP relaxation times, T_{CH}, for carbon atoms in either 3HB or 3HP units virtually resulted from a delicate balance between chemical environment and local mobility. For the 3HP-rich semicrystalline copolyesters, the ^{13}C resonance splitting of CH_2(3HP-α) indicated that the 3HP unit was essential to construct the P(3HP)-type lattice structure, and the contributions ascribed to the crystalline and amorphous regions were explicitly distinguished.

(2) The CP/MAS and PST/MAS experiments revealed that no co-crystallization phenomenon occurs in the bacterial P(3HB-co-3HP)s. The 3HP or 3HB units were entirely excluded from the respective P(3HB)- or P(3HP)-type crystallites, and constituted the amorphous regions with another structural unit.

(3) Besides the results in the crystal morphology and crystallization kinetics as previously reported [11], ^{13}C spin-lattice relaxation experiments suggested that the large difference in molecular mobility between the 3HB and 3HP units may be one more possible reason for the fact that no co-crystallization occurred in the P(3HB-co-3HP) copolyester system.

(4) Lineshape analyses of the 3HB methyl carbon resonances on the fully relaxed DD/MAS spectra revealed that three deconvoluted resonance components could be assigned to the non-crystalline, crystalline and interfacial regions. Even if less amount of the secondary 3HP unit was incorporated, a drastic retarding effect occurred on the crystallizability of the 3HB-rich semicrystalline copolyesters.

(5) The correlation between the average block length of 3HB sequences and crystallizability implied that an L_B longer than two 3HB units was needed for the 3HB-rich copolyesters to form P(3HB)-type crystallites. The 3HB units showed more significantly suppressing effects on the crystallization of the 3HP-rich semi-crystalline

Table 5
Relative intensities of triad sequences determined from the 3HB methine carbon resonances and average block lengths of 3HB sequences for P(3HB-co-3HP)s

Sample code	3HP (mol%)	CH(B) triad relative intensity[a]					
		67.76[b] (B·B·P)	67.69 (P·B·P)	67.61 (B·B·B)	67.56 (P·B·B)	Average block length	
						L_B(exp.)	L_B(calcd.)
AF0	35.4	0.14(0.23)	0.15(0.13)	0.56(0.41)	0.16(0.23)	3.26	2.78
AF1	73.6	0.21(0.19)	0.50(0.54)	0.10(0.07)	0.19(0.19)	1.44	1.36
AF2	60.1	0.21(0.24)	0.41(0.36)	0.15(0.16)	0.23(0.24)	1.57	1.67
AF3	53.1	0.23(0.25)	0.33(0.28)	0.19(0.22)	0.24(0.25)	1.73	1.89
AF4	48.0	0.21(0.25)	0.26(0.23)	0.27(0.27)	0.26(0.25)	1.92	2.08
AF5	38.3	0.21(0.24)	0.19(0.15)	0.39(0.38)	0.22(0.24)	2.47	2.59
AF6	21.9	0.12(0.17)	0.06(0.05)	0.66(0.61)	0.16(0.17)	4.40	4.54
AF7	23.8	0.16(0.18)	0.07(0.06)	0.55(0.58)	0.22(0.18)	3.44	4.17
AF8	15.9	0.12(0.13)	0.03(0.03)	0.70(0.71)	0.15(0.13)	5.56	6.25
AF9	13.2	0.09(0.12)	0.03(0.02)	0.74(0.74)	0.14(0.12)	5.88	7.14

[a] The values shown in parentheses are relative intensities calculated by random statistics.
[b] Chemical shift in ppm from TMS.

copolyesters. This can be rationalized with respect to the different molecular mobility between the 3HB and 3HP units.

Acknowledgements

The authors are grateful to Dr. H. Nishida of Tokuyama Corp. (Tsukuba, Japan) for kindly supplying the chemosynthetic poly(3-hydroxypropionic acid) samples, and for his helpful discussions.

References

[1] Doi Y. Microbial polyester. New York: VCH, 1990.
[2] Inoue Y, Yoshie N. Prog Polym Sci 1992;17:571.
[3] Hocking PJ, Marchessault RH. In: Griffin GJL, editor. Biodegradable polymer. London: Blake Academic & Professional, 1994.
[4] Steinbüchel A, Valentin HE. FEMS Microbiol Lett 1995;128:219.
[5] Anderson AJ, Dawes EA. Microbiol Rev 1990;54:450.
[6] Sharma R, Ray AR. J Macromol Sci Rev, Macromol Chem Phys 1995;C35 (2):327.
[7] Holmes PA, Wright LF, Collins SH. Eur Pat Appl 0 052 459, 1981; Eur Pat Appl 0 069 497, 1983.
[8] Mitomo H, Morishita N, Doi Y. Polymer 1995;36:2573.
[9] Mitomo H, Morishita N, Doi Y. Macromolecules 1993;26:5809.
[10] Yoshie N, Menju H, Sato H, Inoue Y. Macromolecules 1995;28:6516.
[11] Cao A, Kasuya K, Abe H, Doi Y, Inoue Y. Polymer 1988;39:4801.
[12] Fujito T, Deguchi K, Ohuchi M, Imanari M, Albright, M. The 20th meeting in NMR. Tokyo, 1981:68.
[13] Torchia DA. J Magn Reson 1978;30:613.
[14] Ichikawa M, Nakamura K, Yoshie N, Asakawa N, Inoue Y. Macromol Chem Phys 1996;197:2467.
[15] Kitamaru R, Nakaoki T, Alamo RG, Mandelkern L. Macromolecules 1996;29:6847.
[16] Schaefer J, Stejskal EO, Buchdahl R. Macromolecules 1977;10:384.
[17] Mehring M. Principles of high resolution NMR in solid. Berlin: Springer-Verlag, 1983.
[18] VanderHart DL, Perez E. Macromolecules 1986;19:1902.
[19] Komoroski RA. High resolution NMR of synthetic polymers in bulk. FL: VCH, 1986.
[20] Du Prez FE, Goethals EJ, Adriaendens PJ, Gelan JM, Vanderzande JM. Macromolecules 1996;29:4000.
[21] VanderHart DL, Orts WJ, Marschessault RH. Macromolecules 1995;28:6394.
[22] Bluhm TL, Hamer GK, Marschessault RH, Fyfe CA, Veregin RP. Macromolecules 1986;19:2871.
[23] Kamiya N, Sakurai M, Inoue Y, Chujo R, Doi Y. Macromolecules 1991;24:2178.
[24] Yoshie N, Sakurai M, Inoue Y, Chujo R. Macromolecules 1992;25:2046.
[25] Pearce R, Marschessault RH. Macromolecules 1994;27:3869.
[26] Shi F, Richard DA, Richard AG. Macromolecules 1997;30:2521.
[27] Cao A, Ichikawa M, Kasuya K, Yoshie N, Asakawa N, Inoue Y, Doi Y, Abe H. Polym J 1996;28:1096.
[28] Cao A, Ichikawa M, Ikejima T, Yoshie N, Inoue Y. Macromol Chem Phys 1997;198:3539.
[29] Spyros A, Marchessault RH. Macromolecules 1995;28:6108.
[30] Dais P, Spyros A. Prog Nucl Magnetic Resonance Spectrosc 1995;27:555.
[31] Spyros A, Marchessault RH. Macromolecules 1996;29:2479.
[32] Kuwabara K, Kaji H, Horii F, Bassett DC, Olley RH. Macromolecules 1997;30:7516.
[33] Hocking PJ, Marschessault RH. Macromolecules 1995;28:6401.
[34] Hiramitsu M, Doil Y. Polymer 1993;34:4782.
[35] Tian D, Dubois P, Jerome R. Macromolecules 1997;30:2575.
[36] Koubunshi kagaku no kiso (Elementary Textbook of Polymer Science). The Japanese Society of Polymer Science, editors. Tokyo: Tokyo Kagaku Doujin, 1994 (in Japanese).